Image Cover Sheet

CLASSIFICATION	SYSTEM NUMBER
UNCLASSIFIED	146068

TITLE

DUAL ENERGY RADIOGRAPHY: A POTENTIAL CORROSION DETECTION TECHNIQUE

AN: 95-00097

System Number:

Patron Number:

Requester:

Notes:

DSIS Use only:

Deliver to: RL

Defence Research Establishment Pacific
Centre de recherches pour la défense pacifique

DEFENCE RESEARCH ESTABLISHMENT PACIFIC

Research and Development Branch
Department of National Defence

Canada

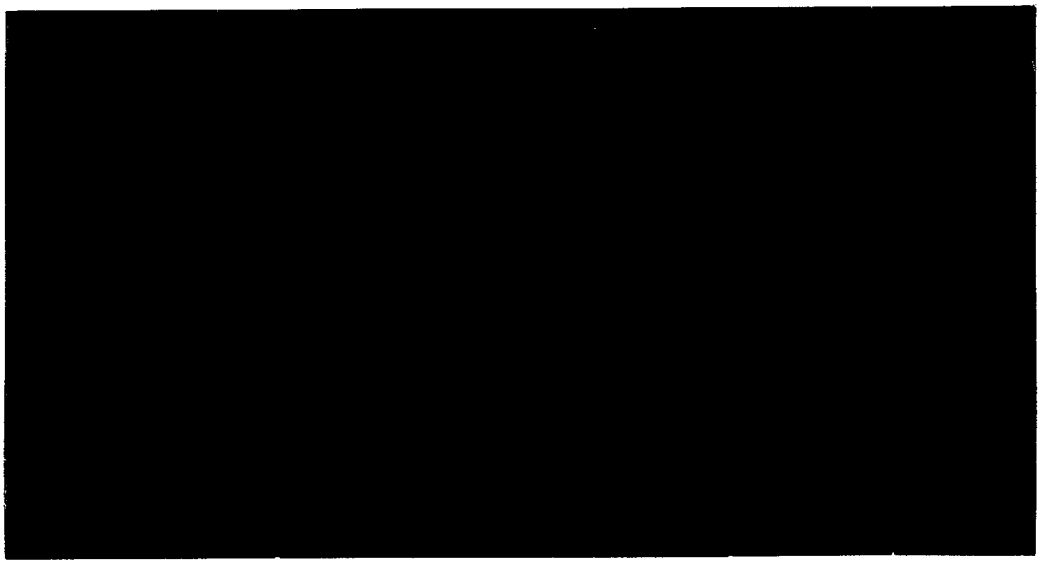

Defence Research Establishment Pacific

Centre de recherches pour la défense pacifique

DEFENCE RESEARCH ESTABLISHMENT PACIFIC

CFB Esquimalt, FMO Victoria, B.C. V0S 1B0

Technical Memorandum 94-05

DUAL ENERGY RADIOGRAPHY: A POTENTIAL CORROSION DETECTION TECHNIQUE

by

SLt J.D. Leblanc and Captain R.D. Finlayson

February 1994

Approved By:

N P Chapman

Chief DREP

Research and Development Branch
Department of National Defence

Canada

ABSTRACT

The recent demand for extending the service life of aircraft fleets well beyond the original design life has made the early detection of corrosion in aircraft a major concern. Consequently, many nondestructive techniques to improve corrosion detection are being investigated. One potential method is known as "Dual-Energy" (DE) radiography and is based on the analysis of two digital radiographs taken at different effective energies. This is achieved by producing two effective radiation energies, either by changing the radiation source energy or by filtering and collecting the radiation from one source via filtered detectors. The information collected from the two digital radiographs can then be combined to form a single digital image that can be used to determine an unknown substance or to remove the effect of a particular substance to improve radiographic contrast.

In this report the theory and concepts of DE are examined and a number of existing systems are discussed. Finally, the possibility of implementing a DE system at the Defence Research Establishment Pacific is investigated.

TABLE OF CONTENTS

1.0 INTRODUCTION

The early detection of corrosion in aircraft structures has become a major challenge for nondestructive testing (NDT) groups. Different systems have been investigated, but none have displayed the desired level of detection required for corrosion. Eddy current systems are good for detecting cracks, pitting, and corrosion occurring at the surface; however, the probability of detection decreases for thicker materials. Also, these systems are rather slow for the inspection of large surfaces. Ultrasonic inspection has proven to be a good detector of delaminations, structural cracks and fractures; however, ultrasonics has difficulties detecting the early stages of corrosion. Ultrasonic inspection systems, like eddy current systems, are also time consuming, requiring many hours to inspect large surfaces. Image enhanced radiographic techniques have been used to detect corrosion; however, an actual loss of material or a change in density must be present in the object for successful detection of corrosion. Material loss only occurs after an extended period of time[1], rendering present radiography systems virtually useless in the detection of corrosion in its early stages. Therefore, it is desirable to develop a radiographic technique that can potentially detect corrosion in its earliest stages of development.

A radiographic image is created from penetrative x-ray or gamma ray radiation which has been modified after passing through an object. The radiation is absorbed and attenuated to varying degrees, as determined by the density of the object. The modified radiation contains a great deal of information about the object's nature, information that is unused with conventional radiographic techniques, information which could potentially improve the radiographic contrast. A promising radiographic technique that could lead to increased detection of early corrosion is to take two digital radiographs at different effective energies either by changing the value of the source energy or by filtering and collecting the radiation of one photon source via filtered detectors. This technique is known as the "Dual-Energy" (DE) radiographic method.

2.0 PRINCIPLES OF DUAL-ENERGY RADIOGRAPHY

In order to better understand DE, it is necessary to review how a photon beam is absorbed in material. DE techniques use particular components from the total linear attenuation coefficient of an attenuated photon beam. The nature of these components and the effects on the photons are described in the following subsection.

2.1 Overview of X-Ray Attenuation

Radiographic images are a representation of the total linear attenuation of the x-ray penetrating radiation (an analogous situation exists for gamma rays). The total linear attenuation coefficient (μ_{total}) for the energy range of 0.1 MeV to 5 MeV is the sum of four components:

$$\mu_{total}=\mu_p+\mu_C+\mu_R+\mu_{pair} \qquad (1)$$

where

μ_{total} : total linear attenuation coefficient
μ_p : photoelectric absorption
μ_C : Compton or incoherent scattering
μ_R : Rayleigh or coherent scattering
μ_{pair} : pair production

The photoelectric absorption affects photons having energy below 1 MeV (see figure 2.1). This process involves a photon incident on an atomic electron. The electron, having completely absorbed the photon's energy, is ejected from its residing state to a higher shell, or may be totally removed from the atom. The empty state is then filled by the return of the excited electron, or by an electron from a higher energy shell (the latter condition is shown in figure 2.2). In any case, both situations will see the emission of a photon with energy characteristic of the electron filling the empty state.

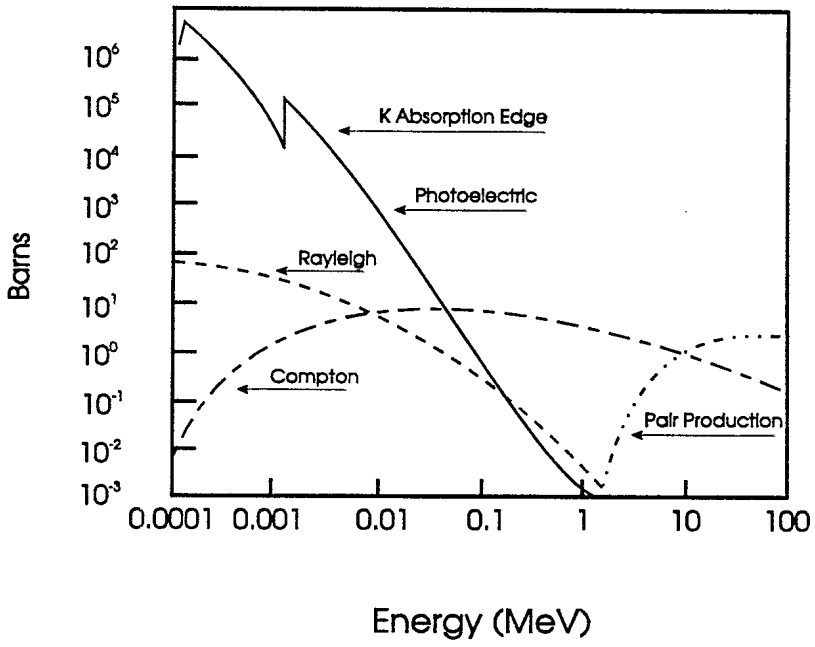

Figure 2.1: Curves of the Various Attenuation Components for Aluminum[2]

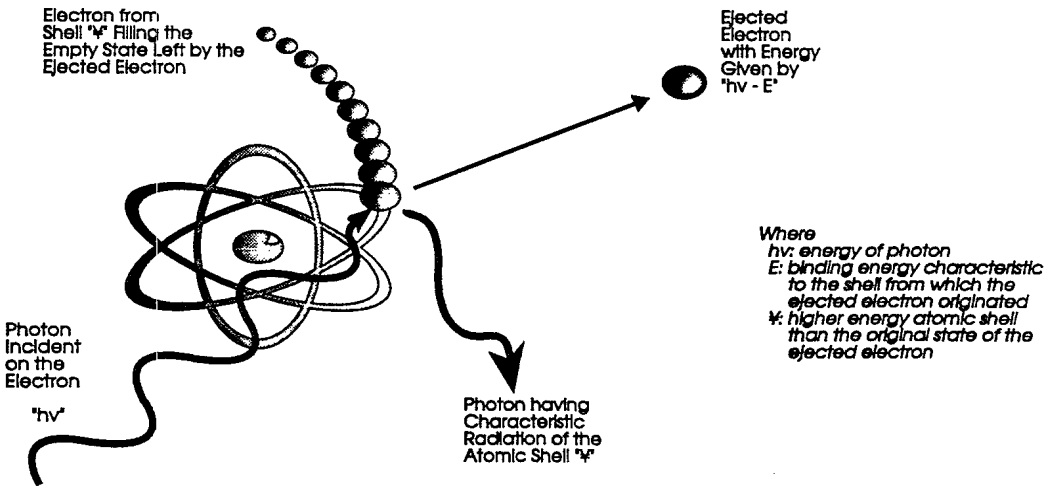

Figure 2.2: Photoelectric Effect

Starting at lower energy and increasing gradually through the energy scale of figure 2.1, the photons are absorbed by electrons lying in states closer to the nucleus, that is the K, L, M, etc. electron shells. The absorption of the photons by these electrons are indicated by sharp increases (absorption edges) in the overall attenuation. The energy required to eject an electron from a state increases as the shell's distance from the nucleus decreases. Accordingly, the K shell being the closest to the nucleus of the atom has its absorption edge located at the higher end of the photoelectric spectrum.

As the photon energy is increased past the K-edge, the main absorption process changes from photoelectric to Compton scattering. This scattering effect contributes to the absorption for photon energies between 100 keV and 5 MeV. Compton scattering is also known as incoherent scattering because the incident photon emerges with a change in energy which occurs when an

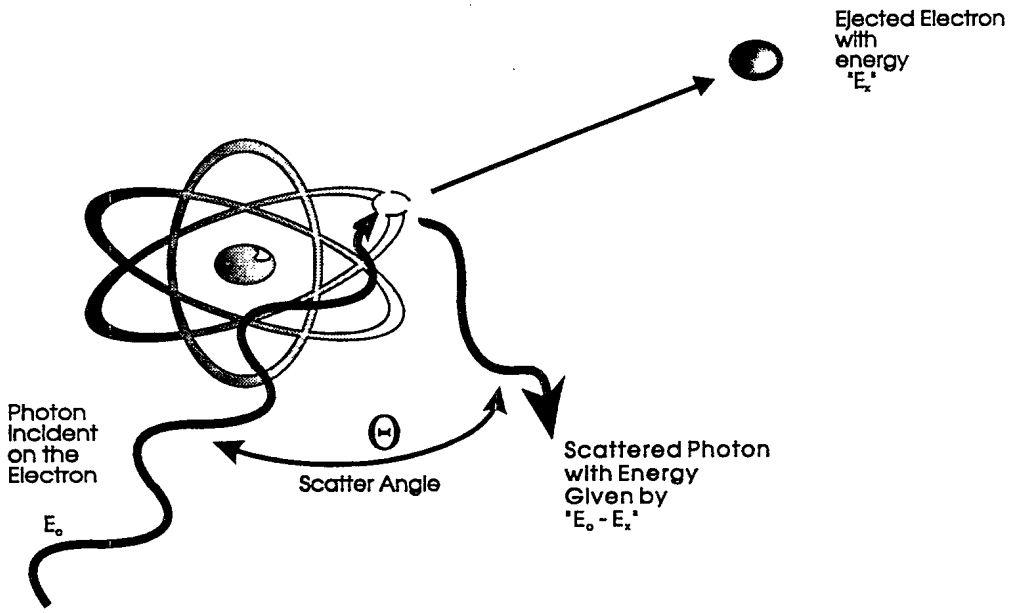

Figure 2.3: Compton or Incoherent Scattering

incident photon transfers only some of its energy to the electron. The initial photon energy must always be greater than the binding energy of the atomic electron. According to the analysis

performed by A.H. Compton[3], the energy shift depends solely on the angle of scattering (θ) and not on the nature of the scattering medium. The larger energy shifts correspond to larger scattering angles of the photons. In the case of a direct hit with an electron, the photon will be scattered backwards at 180°, with a maximum energy transfer to the electron. The effect of Compton scattering on the overall attenuation rapidly reduces as the photon energy is increased over 5 MeV. This is due to the larger penetrating power of the photons, thus diminishing the photon's probability of being scattered by an electron.

The Rayleigh effect produces coherent scattering because the incident photon emerges from the interaction without any change in energy. This type of scattering rapidly decreases as the photon energy increases. In the case of materials with low atomic numbers and photon energies above 100 keV, Rayleigh scattering has a relatively small effect on the total attenuation. The effect of Rayleigh scattering is negligible when compared to the effects of the photoelectric and Compton processes.

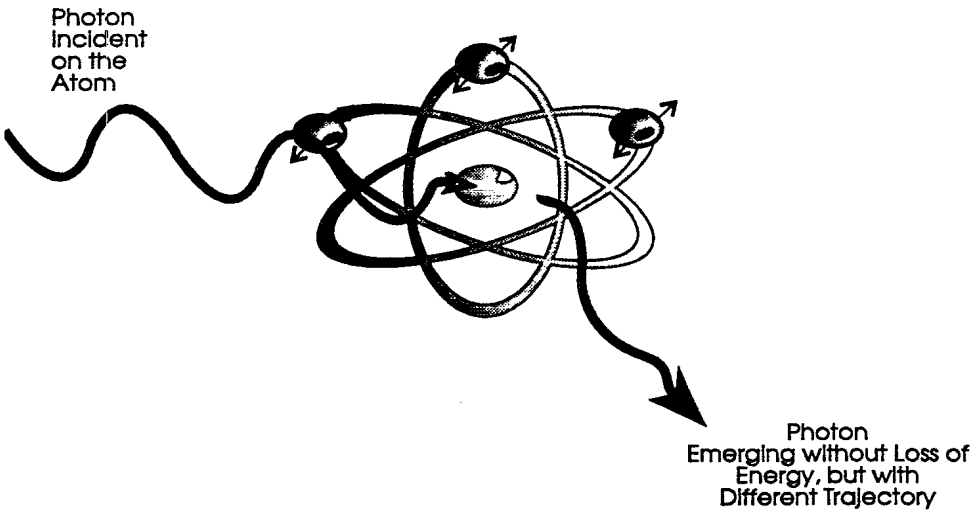

Figure 2.4: Rayleigh or Coherent Scattering

As seen in figure 2.4, Rayleigh scattering occurs when a photon is incident on an atom. The photon is absorbed by the atom, which initiates the oscillation of atomic electrons. The electrons, behaving as a collective source, emit a photon with a frequency identical to the incident photon. The direction of travel of the scattered Rayleigh photons are usually constrained within a small range of angles.

Typical electron energy levels for DE applications are below 200 keV, where the Compton and photoelectric effects are prominent for low atomic number (Z) materials. Because pair production will only occur at very high photon energies (above 1.02 MeV), it can be ignored for DE purposes. Rayleigh scattering has a relatively weaker effect on the overall process, but its presence in the attenuation mechanism cannot be disregarded, and must be treated as a noise problem. For DE analysis the total attenuation coefficient is, therefore, the sum of two terms:

$$\mu_{total}=\mu_p+\mu_C \qquad (2)$$

Because Rayleigh scattering affects both terms shown in equation 2, μ_p and μ_C are not pure photoelectric and Compton terms. The term μ_p is a cross-section generated to best approximate the photoelectric interaction, but is also subject to noise created by the Rayleigh effect. The μ_C term includes the Compton and Rayleigh effects.

2.2 Theoretical Background

The photoelectric and Compton components can be described by the product of two terms:

$$\mu_p=f_p(E)\cdot\varsigma_p \qquad (3)$$

and

$$\mu_C = f_C(E) \cdot \varsigma_C \qquad (4)$$

where

f_c: function depending solely on the energy (E) of the photons

ς_p: spatial dependency for photoelectric and Rayleigh effects

ς_C: spatial dependency for Compton and Rayleigh effects

The function f_c depends exclusively on the energy of the incident photons. The second term ς depends solely on the property of the material under investigation. The spatial dependency terms, ς_p and ς_C, are proportional to the atomic number, Z, and inversely proportional to the local mass number, A, of the irradiated material. The term "spatial dependency" indicates that equations 3 and 4 pertain to only one location within the total volume of the object. In the case of radiography, the location is the actual path taken by the x-ray beam through the targeted matter. Hence this location is not a point or a volume element within the object, but is the value of a line integral. The energy functions f_p and f_C can be solved with predetermined formulae (as described in the appendix to this report, equations 9 and 10). This approach may be used if the x-ray beam's effective energy is known. Although an x-ray source irradiates over a certain energy bandwidth, the effective energy is defined as the peak region of this spectrum. However, for better results the values of the functions f can be determined experimentally. The advantage of this empirical approach is that the resolved values are specific to the system in use.

Substituting equations 3 and 4 into 2, the total attenuation of the beam is then given by:

$$\int \mu_{total}\, dl = f_p \cdot \int \varsigma_p\, dl + f_C \cdot \int \varsigma_C\, dl \qquad (5)$$

where

dl: infinitesimal length partition

The integral signs in equation 5 indicate that the attenuation of the beam is occurring along the entire ray path through the object. The total linear attenuation coefficient μ_{total} can be solved mathematically (see appendix, equation 21); therefore, there are now only two unknowns ς_p and ς_C left to be determined. In order to solve for the two unknowns, two equations must be available to form a square (2 X 2) matrix. The collection of two different spectra (low energy, E_{lo}, and high energy, E_{hi}) provides the data for the two required equations. These equations are of the equivalent form shown by equation 5:

$$\int \mu_{total_{lo}} dl = f_{p_{lo}} \cdot \int \varsigma_p dl + f_{C_{lo}} \cdot \int \varsigma_C dl \qquad (6)$$

and

$$\int \mu_{total_{hi}} dl = f_{p_{hi}} \cdot \int \varsigma_p dl + f_{C_{hi}} \cdot \int \varsigma_C dl \qquad (7)$$

These equations show that the spatial terms (ς) are totally independent of the energy irradiated, therefore, suggesting the square matrix can be solved by a linear method. These terms are solved for all points (pixels) within the digital image. Once solved, the pair of spatial data forms two basis images: the photoelectric and the Compton images. These basis images depend solely on the properties of the material under investigation. The photoelectric data is proportional to the density (ρ) and the atomic number raised to the fourth power (Z^4), whereas the Compton data is proportional to the values of ρ and Z of the irradiated material. If equations 6 and 7 were drawn on an X-Y axis, the two functions would have to intersect (known as linear independence) in order to be able to solve for the spatial terms. A critical selection of the energy values (E_{lo} & E_{hi}) must be made, in order to produce this greatest degree of linear independence between the two equations. The energy selection is also dictated by the radiographic system specifications, including the energy dependent efficiency of the x-ray detector used and the noise in the system[4]. Therefore, E_{lo} and E_{hi} are chosen not only to fulfil the mathematical requirement, but are also limited by the available hardware.

Although the basis images contain important information on their own, further mathematical operations can produce a powerful application, known as artificial cancellation. This technique is used to cancel the features of a chosen material from a radiographic image. The cancellation of a specific material (as determined by Z) is achieved by performing a weighted subtraction of the two basis images:

$$k_p \cdot \int \varsigma_p dl - k_C \cdot \int \varsigma_C dl = 0 \qquad (8)$$

By manipulating equation 8, the ratio of the weight factor (k_C/k_p) is then made proportional to Z^3 of the material which is to be artificially cancelled from the image.

$$\frac{k_C}{k_p} = \frac{\int \varsigma_p}{\int \varsigma_C} \propto \frac{\rho Z^4}{\rho Z} = Z^3 \qquad (9)$$

Since one value of Z is chosen, the proportionality shown in equation 9 can be true for only one type of material. The digital cancellation can then occur for only one element or compound per process. A diagram of the overall DE process including artificial cancellation is shown in figure 2.5

Consider an aluminum piece subjected to oxidization. An NDT technician could remove the effects due to aluminum in order to see the corrosion on the video display. The DE technique can have many applications other than corrosion detection. In the case of a complex specimen being irradiated, the cancellation of a chosen element could make it easier to detect the presence of foreign objects. DE radiography could also be used to detect contamination in fuel; cancel all materials other than gaskets or seals in order to inspect their integrity; screen for missing components; inspect for delamination; or produce an overall contrast improvement.

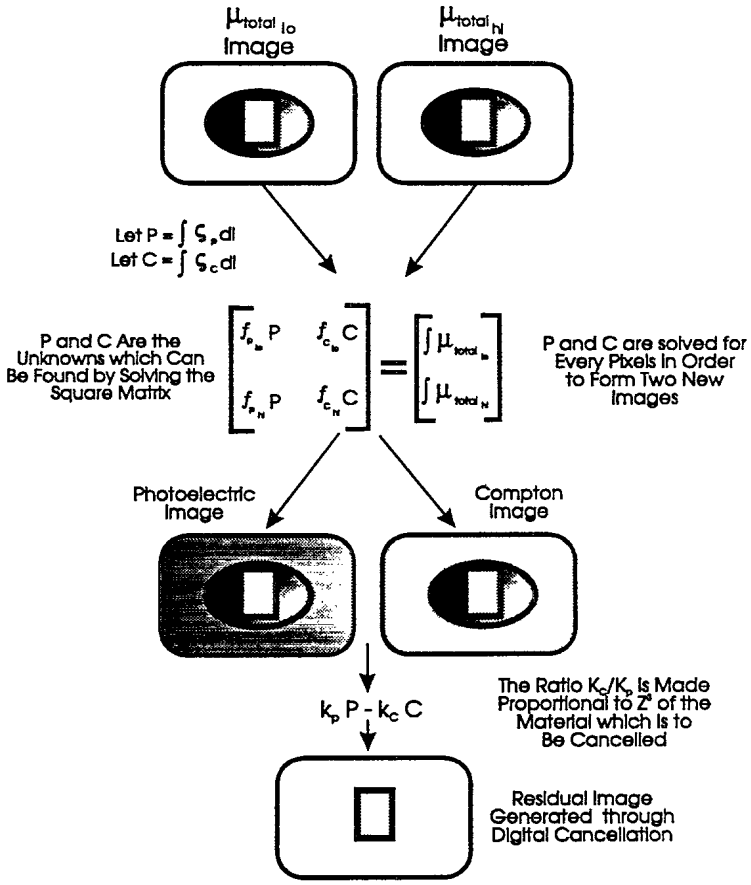

Figure 2.5: Dual-Energy Process for Digital Cancellation

3.0 THE HISTORY AND DEVELOPMENT OF DUAL-ENERGY RADIOGRAPHY

The development of DE techniques occurred over two periods: 1) the "early period" where analog computers and film radiography systems were the dominant methods in use, and 2) the more recent "digital period" which has seen an increasing number of radiographic systems utilizing fast digital processing units.

3.1 The Early Period

DE radiography is not a new idea. In 1925, K edge techniques were used by Glocker and Frohnmayer[5]. This method can be used to improve the contrast of a single given element. Photon absorption from the ejection of electrons residing in the K shell has been briefly discussed in section 2.1. Consider functions representing the linear attenuation coefficients of three elements (see figure 3.1).

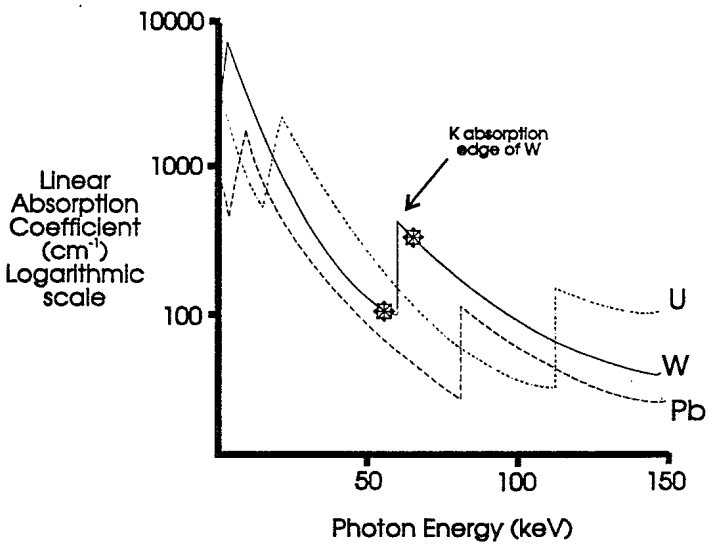

Note: The Attenuation Curves presented are approximated

Figure 3.1: Linear Attenuation Coefficients of Three Elements at Low Photon Energy Including K-Edge Absorption

Figure 3.1 shows that the K absorption edge occurs at distinct photon energies for different elements. In the example, a material is composed of three basic elements; lead (Pb), tungsten (W), and uranium (U). In order to improve the contrast of tungsten, the exact location of the K edge within the energy spectrum must be known. The technique involves taking measurements of the transmitted radiation just below and above the tungsten's K edge (shown

by the stars in figure 3.1). A large variation in absorption for W can be detected between the two measurements. This absorption difference is much greater for tungsten at energies around 60 keV, than for the Pb and U constituents. If the two measurements are taken as close to tungsten's K edge as allowed by the system in use, then the differences in absorption for Pb and U will be minimal. Consider a set of two images generated from the data taken by these two measurements. The only large variation between the two images would be produced by the tungsten, whereas the remaining features would practically be identical. Subtracting the two images then would cancel all identical features, thus revealing an enhanced tungsten contrast.

DE methods, including K edge techniques, could not be practically implemented prior to the 70's. One of the main limiting factors in the performance of the source/detector system was the signal-to-noise ratio (S/N). Designers had to estimate many factors affecting the S/N: these included the absorption path, the imaging energies, and the digitally cancelled material[6]. The noise problem was also coupled with the issues of the Rayleigh scattering present in the cross-section terms, and the matching of these terms to μ_{total}. The problems with the accuracy of the numerical method required to manage the noise, and slow computer processing speeds, were not to be solved until the arrival of the 1980's, with the availability of workstations and personal computers.

3.2 The Digital Period

The rapid advances in digital image technology and computer processing time have made the construction of a working K edge system feasible. Such a system has been developed at the University of Wisconsin[7] with a rotating triple filter, providing the option of choosing dual or triple energy radiography (see figure 3.2).

In this system x-rays are produced in short bursts in order to keep the patient dose to a safe level. The kVp used in this system ranges between 30 and 55 kVp. These radiated bursts are synchronized by the logic system to correspond with the speed of the rotating wheel. Thus, different beam intensities can be matched to one of the three filters available. An appropriate

choice of intensities and filters will accurately locate the photon energies, below and above the K edge of the organic tissue under investigation (for example, a brain scan could be K edge processed, where iodine contrast would be enhanced against a background of uniformly cancelled bone and tissue residuals). The system uses an image intensifier and video camera to detect the photons. The analog signal is then digitized and the image processing is performed by a digital processor which is fast enough to perform data accumulation, storage, and real-time operations.

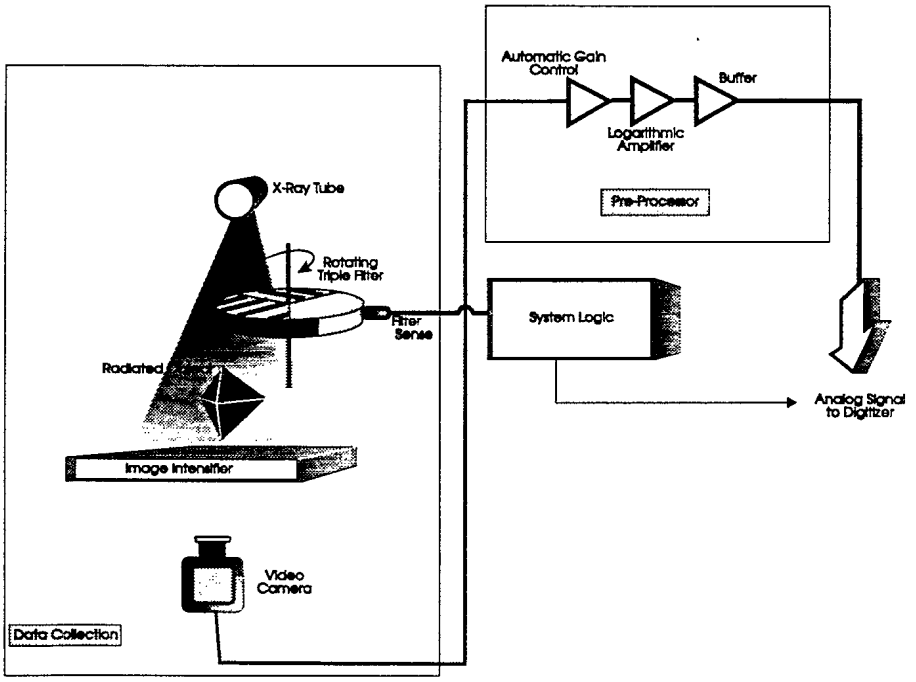

Figure 3.2: Digital Video Image Processor for K-Edge Subtraction Imaging

In situations other than medical or clinical applications, the technique described above has a limited effectiveness. For the K edge techniques to be effective, the exact location of the desired edge within the photoelectric effect curve must be known. In the case of an aircraft or ship, the multitude of elements, compounds and composites present limits the usefulness of K edge techniques. Also, K absorption is the result of the photoelectric process only, whereas the

DE radiographic method includes the photoelectric and Compton components from the total linear attenuation coefficient. Hence, the DE technique described in section 2 has evolved into the method of choice for NDT applications.

3.3 Dual-Energy Systems

There are two basic requirements for a radiographic system to be capable of using the dual-energy technique. First, a high and low energy digital radiograph must be taken, either via an adaptable x-ray tube output rating, or by filtering and collecting the radiation of one photon source through filtered detectors. Secondly, the digitized data must then handled by a digital image processor which must operate in real-time or near real-time. The simplest method to produce DE radiographs involves irradiating the targeted object at two different energies.

Most systems are DE capable if the accelerating voltage can be adjusted over a range of 200 kV to 450 kV. Two ordinary x-ray tubes could be used if they are rated within the described energy range. In this instance, the x-ray tubes may have to be physically changed between the two scans. This procedure could create a problem, as the physical location of the irradiated object with respect to the radiographic system must be identical for both scans. If the same location is not maintained, artifacts will be created, reducing the contrast gained by using a DE technique. The use of a linear array detector as shown in figure 3.3 produces data that can be digitized, however, any detector generating data which can be readily digitized is DE compatible, including image intensifiers, digital linear arrays, and solid state crystal detectors. Figure 3.3 shows an example of a medical system, where the subject is placed on a moving table, and translated through a stationary fan beam. For NDT applications, the object under analysis could be secured from movement while being scanned by a source located in a mobile gantry.

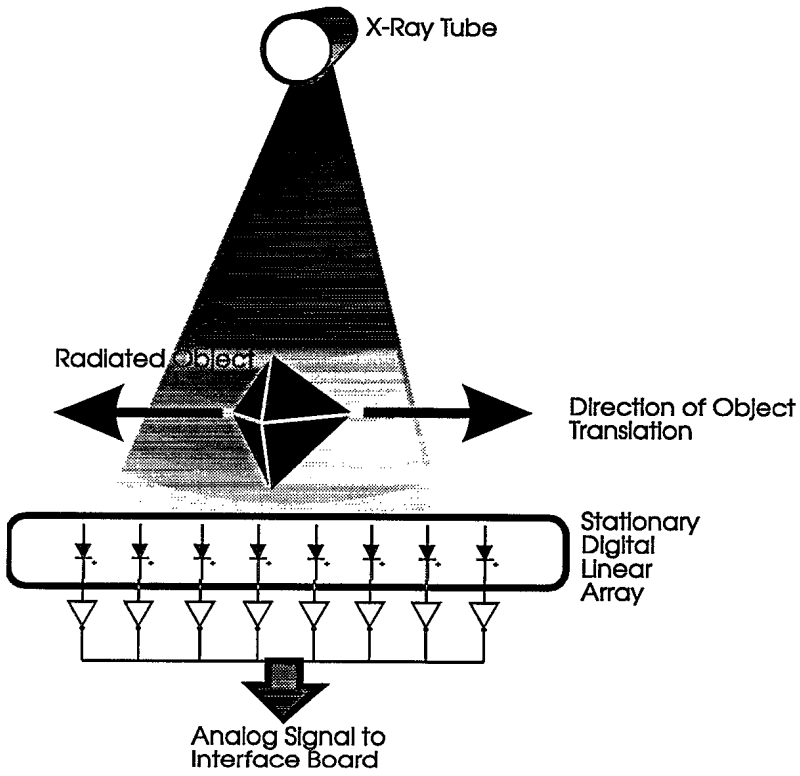

Figure 3.3: Linear Array Detector

To eliminate the problem of using two x-ray tubes, techniques involving only one exposure were developed. A single DE scan can be performed by pulsing the x-ray beam between two different energies at a predetermined frequency. Hall et al.[8] successfully demonstrated such a system, generating the two levels at different pulse widths and alternating at a rate of 60 Hz (see figure 3.4). This system was developed primarily for medical research, taking into account the maximum dosage that a patient can safely receive. The low energy pulse has a width of 3.3 ms with a peak of 85 kVp, while 135 kVp is radiated with a pulse width of 5.5 ms for the high energy beam. Currents of 1000 mA and 250 mA, respectively, are applied to the tube. The scan from this system is divided into E_{lo} and E_{hi} data, then mathematically processed for the formation of the basis images.

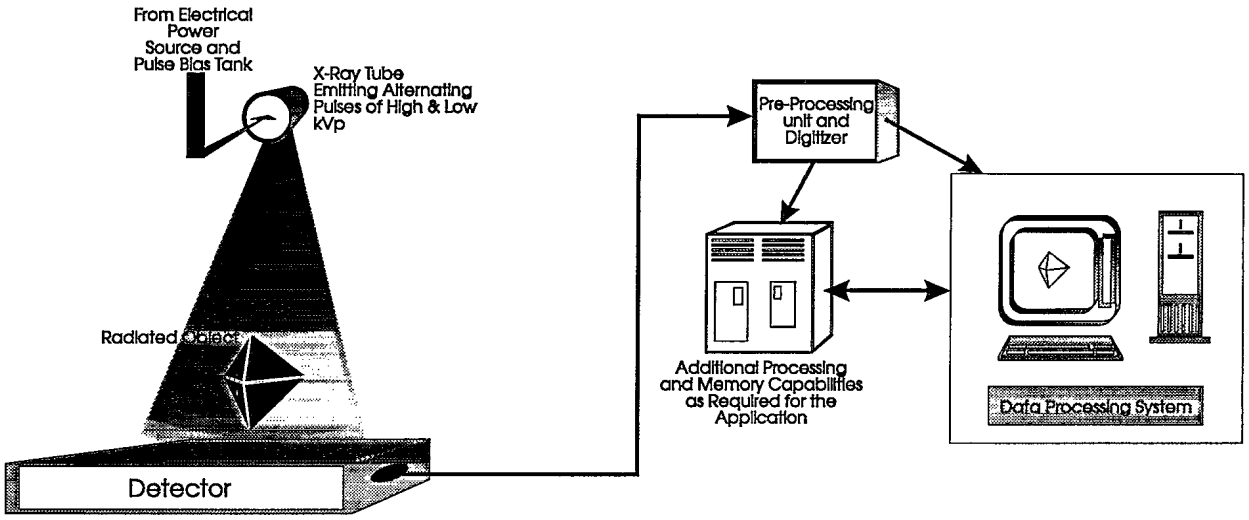

Figure 3.4: Characteristic Dual-Energy Implemented by Pulsed Radiation

While conceivable for use in the medical field, the short pulsed radiation provided by this method would be unacceptable for the inspection of metals. Extending the pulse length, however, would allow nondestructive testing of heavier non-organic materials. Longer pulse lengths necessitate a slower scanning speed, to ensure that the E_{lo} and E_{hi} images have complete data sets.

Another DE system that has been developed is shown in figure 3.5. This system collects two spectra per exposure, via a xenon charged detector tube. The detector is made up of four plates: two exterior high voltage electrodes made of tantalum, alternating with two collector plates fabricated from double-sided epoxy circuit boards. This system can be used in two different configurations: the front-back or the high-low method. Both methods can be used for cancellation; however, from his studies, Fenster[9] determined that the high-low method proved more accurate in yielding values of density (ρ) and mean atomic number (Z). The front-back method consists of a front detector which receives mainly low energy photons, and a back detector that receives the high energy photons. The low energy photons have primarily interacted with the irradiated object through the photoelectric process, whereas the high energy photons have been mainly scattered via the Compton process. The high-low method uses the same basic

idea as the front-back, but introduces the following ratios:

$$L = f \cdot (F + B) \tag{10}$$

and

$$H = (1 - f) \cdot (F + B) \tag{11}$$

where

f: fraction of the total energy in the x-ray beam emerging from the attenuator

F: front detector signal

B: back detector signal

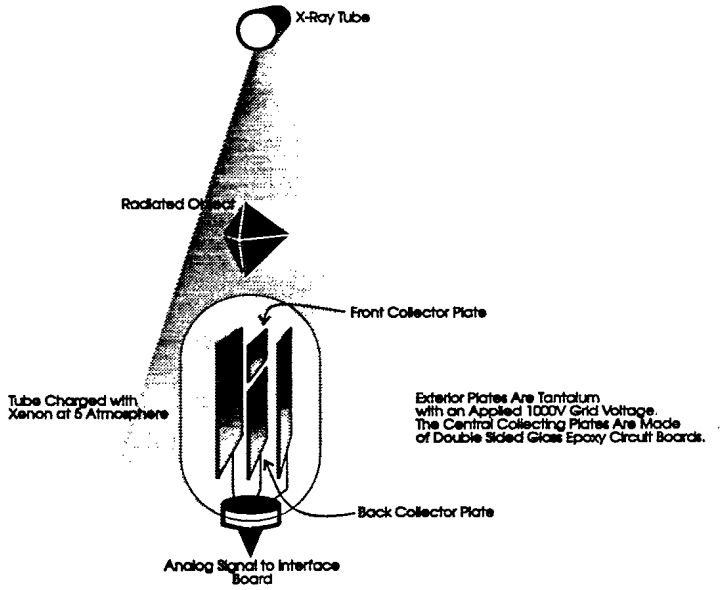

Figure 3.5: Split Xenon Detector

Assuming that attenuation is due only to the photoelectric and Compton processes, the fraction, f, can easily be transformed into any required value, determining mathematically the division between the high and low photon energies. In other words, the high-low configuration

allows the user to choose the energy boundary, which cannot be done with the front-back method. Recall that the principal absorption process changes from the photoelectric to the Compton process, as the photon energy is increased past the K edge; therefore, the "f" value would then be set to locate the boundary slightly above the energy required for K edge absorption. For example, consider an energy spectrum ranging between 0 and 200 keV. If "f" is chosen to be 25%, then the boundary would be set at 50 keV. Considering equation 10 and the example given above, L would be the fraction of the spectrum detected by the collector plates determined by photons with energy less than 50 keV, basically corresponding to the photoelectric effect. For equation 11, H would represent the portion of the spectrum with energy greater than 50 keV, corresponding to photons that result from the Compton process.

Advanced Research and Applications Corporation (ARACOR) of California has worked with DE techniques applied to NDT since the early 1980's, and has developed a LAMinography/Dual-Energy (LAMDE) prototype[10,11]. Their system evolved from a standard x-ray set up, to one specifically designed to meet the requirements of DE. Throughout the design process, LAMDE acquired the two spectra by performing only one individual scan. The system was designed to operate with a single photon source, radiating at a predetermined kVp. The collection of the E_{lo} and E_{hi} spectra was achieved through filtered detectors. An early design consisted of a linear array made up of 64 dual in-line detector elements (see figure 3.6). Each channel was composed of a brass filter sandwiched between a pair of front and back detectors. The detector bank consisted of 64 individual channels situated side by side. The active detector elements included in the package were photodiodes. Later, a newer Computed Tomography (CT) design was implemented, which allowed substitution of the filters depending on the nature of the radiated material[12]. This subsequent system was calibrated with an accelerating voltage of 420 kV for E_{hi}, and an E_{lo} ranging between 250 and 320 kV. The calibration process also took into consideration the Rayleigh effect on the two cross-section terms (μ_p and μ_C). For NDT applications, the Rayleigh scattering has a definite significance due to the heavier elements and compounds being tested.

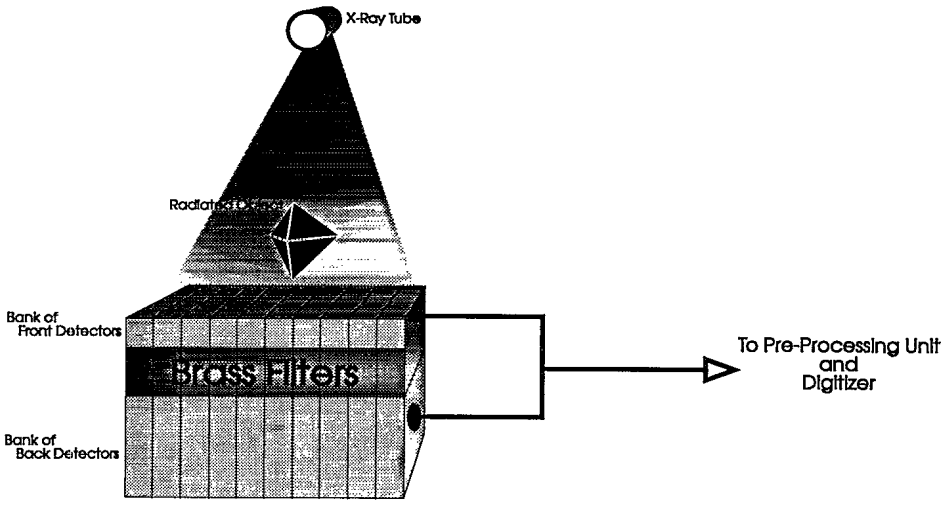

Figure 3.6: Simplified Diagram of the LAMDE System

4.0 FEASIBILITY OF IMPLEMENTING DUAL-ENERGY RADIOGRAPHY AT THE DEFENCE RESEARCH ESTABLISHMENT PACIFIC (DREP)

The Nondestructive Evaluation Group at DREP already possesses some of the hardware needed for DE radiography. Many photon sources with different irradiating energies are available, and x-ray detection can be performed by the linear array or the image intensifier systems. Once an x-ray source and detector configuration has been chosen, the system must be integrated to an individual computing station. Calibration of the radiographic system is then performed, in order to find the energies (E_{lo} & E_{hi}) required to achieve the greatest degree of linear independence, and the related energy functions (f_p & f_C). A test sample must be irradiated during the calibration, which is representative of the atomic numbers corresponding to the expected range of the materials to be investigated. As mentioned in earlier sections, this calibration is not exclusively for hardware adjustment, but to generate the optimum match of the cross-section terms.

Tests were implemented in order to determine the suitability of DREP systems for DE.

The tests involved:

a) detecting the initial beam intensities (I_o);

b) determining the best detector medium for DE purposes;

c) producing the data manipulation program; and

d) determining the feasibility for material cancellation with a pure theoretical approach.

As described in the appendix to this report, a means of measuring the photon beam intensity at the source (I_0) and also the attenuated beam intensity at the detector (I) is required. Ideally, each pixel forming the data matrix has to be sampled without any object located between the source and the detector. With this method, I_0 should be greater in the middle of the matrix than the values recorded by the active elements located at the edge of the detector package, provided that the source and the detector have been properly aligned. Once an object is irradiated, each pixel would be paired for its I_0 and I values, however, in order to facilitate the process, the average value of the pixel matrix was calculated and used as the I_0 value. It was found that the actual I_0 magnitude did not vary by more than 3 grey levels (from a 255 grey scale) throughout the entire data matrix. Then, the initial intensity was measured by irradiating the detector (linear array, or image intensifier) without a test object placed in the beam path.

The image intensifier was evaluated to determined its compatibility with the approach discussed above. The technique used required a steady frame of reference to obtain a valid I_0 value. The image intensifier produced a large variation in pixel values between frames. Thus, the real-time nature of the image intensifier made it difficult to "grab" a steady initial data frame.

The linear array proved to be more manageable for the experiments. The overall pixel values were more stable across the entire image created by the array (difference of 3 grey levels between lowest and largest data value). Also, higher drive current could be used with the linear array before saturation was reached. One drawback of the linear array was the limitation to a maximum allowable x-ray tube accelerating voltage of 160 kV. As described earlier, grid voltages ranging between 200 kV and 450 kV are desirable for successful NDT applications.

To perform a practical DE test, a graphite and titanium steplap joint was then introduced (see figure 4.1). Graphite has a negligible photoelectric contribution to x-ray absorption above 100 kV. On the other hand, the photoelectric contribution is a significant component of titanium's x-ray absorption. In addition, the atomic number range applicable to NDT situations is covered by the two materials of the sample. DREP has an x-ray tube that can be operated over an energy range of 200 kV to 450 kV; however, due to the energy limit set by the linear array, film radiography had to be used to collect E_{hi}, 420 kV and E_{lo}, 300 kV. Proofs of the two negatives were made by contact printing, then scanned at a resolution of 300 dots per inch for digitization. Although this process does not fulfil the real-time requirement and reduces the overall resolution, it was used to overcome the problem caused by the lack of detector suitable for high energy photon sources. The basis images generated can be seen in figure 4.2. Figure 4.2.b shows the photoelectric data and Figure 4.2.c the compton data. Artificial cancellation using the basis image was not successful, due to inappropriate energy functions, f_p & f_C not taking into account the effect of Rayleigh scattering. Also, an algorithm was not developed to correct for the apparent change in thickness around the edges of the sample, caused by the different angles of incidence. In order to improve on the method evaluated a better method of determining I_o values for every pixel would be required.

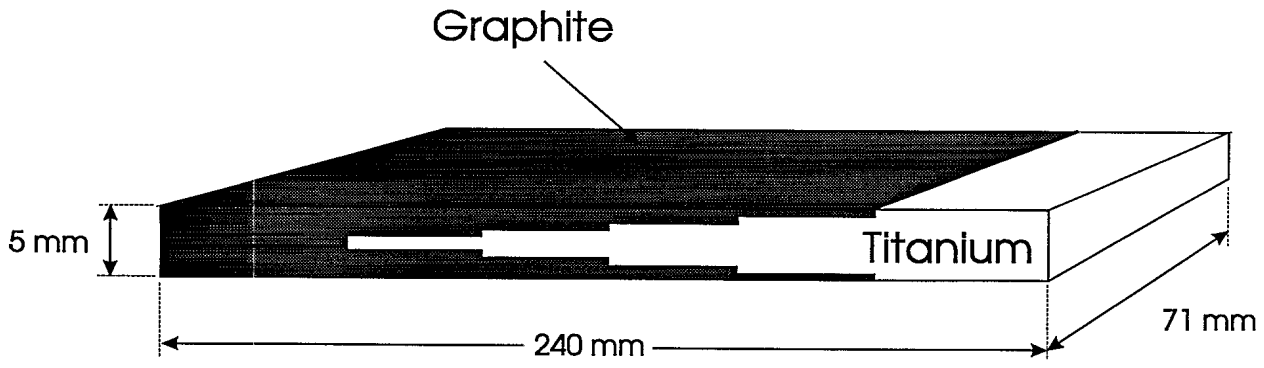

Figure 4.1: Titanium - Graphite Sample

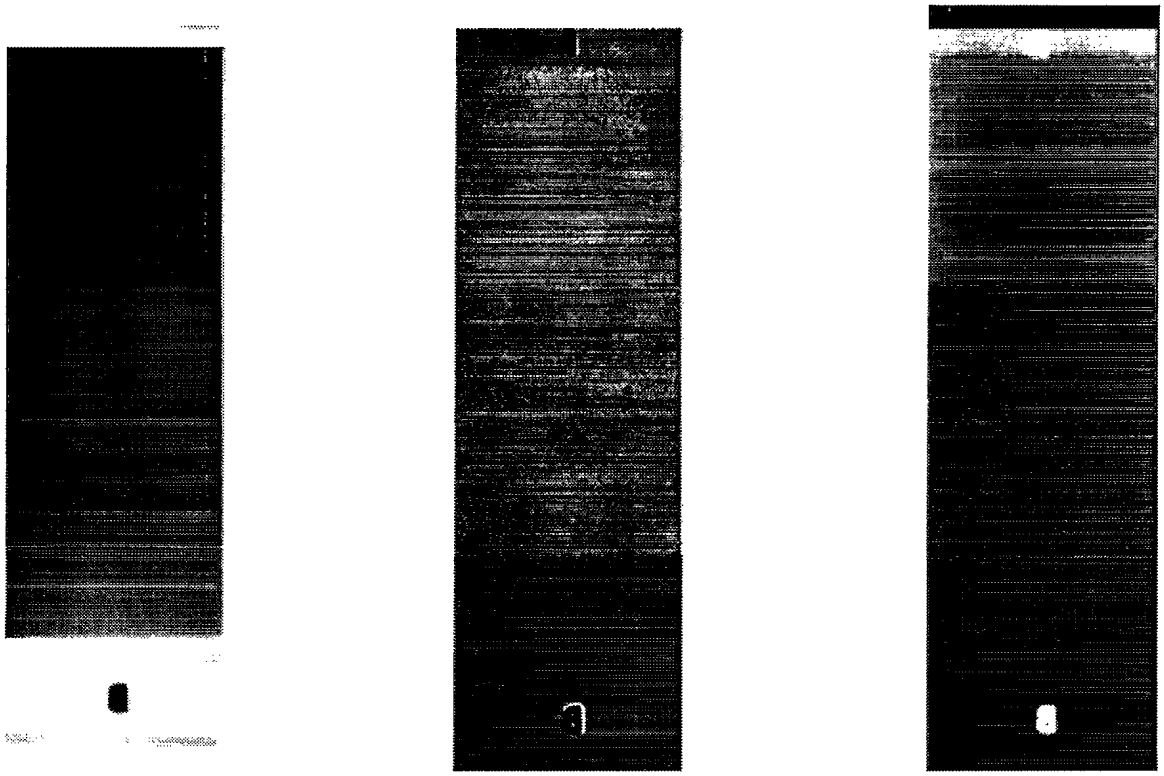

a) E_{hi} Radiograph

b) Photoelectric image

c) Compton Image

Figure 4.2 Radiographs produced from the dual energy technique using film. E_{hi} is 420 kV an E_{lo} is 300 kV.

5.0 CONCLUSION

The DE radiographic techniques have two positive aspects when compared to single energy radiography: the contrast is augmented by artificially cancelling the presence of materials of a known element within the image, and the average atomic number (Z) as well as the electron density (ρ) can be calculated for each pixel.

The technique has some drawbacks since the features of only one material may be digitally suppressed at a time, and the total cancellation of a substance will remove some of the desired contrast. For the case where an object is made of many elements, the cancellation of

only one of these may not create a great improvement in the contrast. Also, extensive calibration of the radiographic system must be performed to cover the considerable range of material type. Finally, there is a requirement for high energy photon sources and detectors (up to 500 kV).

The inclusion of the external and system noise, Rayleigh effect, and the extended range of atomic numbers seen in NDT applications make it difficult to strictly adhere to the theoretical pattern. These problems indicate that even if the theoretical model can be applied to many radiographic systems, the specifications of a particular system must be adequately studied and included in the overall design. A system specifically designed for DE application, obtaining the two spectra via a single scan, as built by ARACOR, would certainly improve the overall results. To further improve the results, an operator must be trained to analyze the images in order to empirically adjust the ratio of photoelectric and Compton images (ς_p and ς_C). The operator must also have a considerable experience with the system to make it a viable technique and improve its accuracy.

6.0 RECOMMENDATIONS

Further research into dual energy radiography is not recommended at this time. The high levels of energy required to perform the technique are not acceptable for field use in the Canadian Forces. However, as the dual energy technique shows promise, it is further recommended that as research continues in the private sector the Canadian Forces periodically review its progress. At such time that DE can be performed with lower energy levels the CF should re-evaluate the technique with a view to possible CF use.

REFERENCES

1. Wallace, W., and Hoeppner, D.W. "Aircraft Corrosion: Causes and Case Histories" AGARD Corrosion Handbook vol 1, AGARD-AG-278, *AGARD*, (1985).

2. Plechaty, E.F., Cullen, D.E., and Howerton, R.J. "Tables and Graphs of Photon-Interaction Cross Sections from 0.1 keV to 100 MeV Derived from the LLL Evaluated-Nuclear-Data Library", *Lawrence Livermore Laboratory*, 61, (1981).

3. Compton, A.H., and Allison, S.K. "X-Rays in Theory and Experiment", D. Van Nostrand Company, Inc. New York, (1935).

4. Riederer, S.J., Kruger, R.A., and Mistreatta, C.A. "Limitations to Iodine Isolation Using a Dual Beam Non-K-Edge Approach", *Med. Phys.*, 8, no. 1, 54-61, (1981).

5. Alvarez, R.E. "Extraction of Energy-Dependent Information in Radiography", Ph.D. Thesis, *Dept. Elec Engr., Stanford University,*p. 4-5, (1976).

6. Lehmann, L.A., and Macovski, A. "Noise and Material Residues in Dual-Energy Basis Decomposition Radiography", *Digital Radiography*, 314, 143-148, (1981).

7. Kruger, R.A., Mistretta, C.A., et al. "A Digital Video Image Processor for Real-Time X-Ray Subtraction Imaging", *Optical Engineering*, 17, no. 6, 652-657, (1978).

8. Hall, A.L., et al. "Experimental System for Dual Energy Scanned Projection Radiography", *Digital Radiography*, 314, 155-159, (1981).

9. Fenster, A. "Split Xenon Detector for Tomochemistry in Computed Tomography", *Jour. of Compt. Asst. Tomogr.*, 2, 243-252, (1978).

10. Stanley, J.H., and LePage, J.J. "A New Radiographic Corrosion Inspection Capability", *Air Force Wright Aeronautical Laboratories*, AFWAL-TR-85-4130, (1986).

11. Yancey, R.N., and Stanley, J.H. "A New Radiographic Corrosion Inspection Capability", *Air Force Wright Aeronautical Laboratories*, AFWAL-TR-88-4234, (1988).

12. Stanley, J.H., and Peck, H.E. "Exploitation of Advanced X-Ray Computed Tomography Technology" vol 1, phase 1 of Dual Energy Computed Tomography, *Air Force Wright Aeronautical Laboratories*, AFWAL-TR-88-4018, (1988).

13. Alvarez, R.E. "Extraction of Energy-Dependent Information in Radiography", Ph.D. Thesis, *Dept. Elec Engr., Stanford University,* (1976).

14 Alvarez, R.E., and Macovski, A. "Energy-Selective Reconstructions in X-Ray

Computerized Tomography", *Phys. Med. Biol.*, 21, no. 5, 733-744, (1976).

15. Macovski, A., et al. "Energy Dependent Reconstruction in X-Ray Computerized tomography", *Comput. Biol Med.*, 6, 325-336, (1976).

16. Alvarez, R.E., and Macovski, A. "Noise and Dose in Energy Dependent Computerized tomography", *Opt. Inst. in Med.*, 96, 131-137, (1976).

17. Stanley, J.H., and LePage, J.J. "A New Radiographic Corrosion Inspection Capability", *Air Force Wright Aeronautical Laboratories*, AFWAL-TR-85-4130, (1986).

18. Alvarez, R.E., and Seppi, E. "A Comparison of Noise and Dose in Conventional and Energy Selective Computed Tomography", *IEEE Transactions on Nuc. Sci.*, 26, no. 2, 2853-2856, (1979).

APPENDIX: Mathematical Principles

In this section the mathematical principles and equations required to perform dual-energy analysis will be addressed.

Note: *The following principles were derived using the theory presented in various papers*[13-18].

The total attenuation experienced by a x-ray beam travelling through matter is the sum of all the known interactions and is expressed mathematically in equation (1).

$$\mu(E,Z,A)=\sum_{i=1}^{N}\mu_i(E,Z,A) \qquad (1)$$

where

μ : attenuation

E : x-ray energy

Z : local atomic number

A : local mass number

N : number of different types of attenuation

However, for radiation at relatively low energies (below 1 MeV), only two interaction processes are predominant; the photoelectric effect and Compton scattering. A second type of scattering known as Rayleigh also plays a minor role in the total attenuation.

Equation (1) can therefore be simplified to:

$$\mu(E,Z,A)\approx\mu_1(E,Z,A)+\mu_2(E,Z,A) \qquad (2)$$

Or

$$\mu(E,S) \approx \mu_p(E,S) + \mu_c(E,S) \tag{3}$$

where

μ_p : photoelectric interaction

μ_c : Compton interaction

S : locality

The locality S is the actual position where the beam was attenuated within the radiated object. In theory, the photoelectric and Compton terms should be totally independent, but the Rayleigh effect is inherent in both predominant attenuation terms. The Rayleigh component cannot be subtracted from the Compton and photoelectric terms, and must be addressed as a noise problem. The extent to which the Rayleigh effect contributes to the scattering is a function of the local atomic number, and energy of the photons. With proper calibration, a DE system can account for a large portion of this detrimental effect. If the noise is not addressed properly then any advantage produced by the dual energy process will be lost.

The attenuation terms of equation 3 can be further described by:

$$\mu_p(E,S) = N(S) \cdot \iota_p(E,S) \tag{4}$$

and

$$\mu_c(E,S) = N(S) \cdot \iota_c(E,S) \tag{5}$$

where

N(S) : number of atoms per unit volume (see equation 6)

ι_p : photoelectric atomic interaction cross section (see equation 7)

ι_c : Compton atomic interaction cross section (see equation 8)

The components of equations 4 and 5 are:

$$N(S)=\frac{N_o\rho(S)}{A(S)} \tag{6}$$

where

N_o : Avogadro's number

$\rho(S)$: local material density

A(S) : local mass number

$$\iota_p(E,S)=a_pZ^4(S)f_p(E) \tag{7}$$

and

$$\iota_c(E,S)=a_cZ(S)f_c(E) \tag{8}$$

where

a_p & a_c : dimension-carrying constant independent of photon energy or material composition

f_p : energy dependency of the photoelectric interaction defined as:

$$f_p=\frac{1}{E^3} \tag{9}$$

f_c : energy dependency of the Compton interaction

defined by the Klein-Nishina function:

$$f_c(E)=\frac{1+\alpha}{\alpha^2}\left\{\frac{2(1+\alpha)}{1+2\alpha}-\frac{1}{\alpha}\ln(1+2\alpha)\right\}+\frac{1}{2\alpha}\ln(1+2\alpha)-\frac{1+3\alpha}{(1+2\alpha)^2} \quad (10)$$

where

$$\alpha=\frac{E}{510.975keV} \quad (11)$$

Note: *for a polychromatic source (containing more than one wavelength), E has to be interpreted as the effective energy of the x-ray beam. The energy formulae (f_p & f_C) reproduced above are purely theoretical, where the Rayleigh effect has not been included. Empirical results obtained through system calibration would considerably improve the method for NDT applications.*

Therefore

$$\mu_p(E,S)=\frac{N_o\rho(S)}{A(S)}a_pZ^4(S)f_p(E) \quad (12)$$

and

$$\mu_c(E,S)=\frac{N_o\rho(s)}{A(S)}a_cZ(S)f_c(E) \quad (13)$$

One of the advantages of dual energy radiography is that the different attenuation terms

are proportional to the average atomic number of the material.

$$\mu_p(E,S) \propto \rho(S) \cdot Z^3(S) f_p(E) \tag{14}$$

and

$$\mu_c(E,S) \propto \rho(S) f_c(E) \tag{15}$$

Note: *Z/A is approximately constant over the entire periodic table (approximately ≃ 0.474 for 2≤Z≤20). However, many anomalies occur within the periodic table including:*

1. Z/A for hydrogen = 1,

2. Some low Z compounds (composed of low Z elements), like corroded organic or inorganic material have Z/A ≃ 0.5, and

3. Z/A for 20<Z<30 ≃ 0.46.

Equations (12) and (13) can be abbreviated to two components: one representing the spatial dependency of the material, followed by the energy dependent function. The spatial dependency components are defined as:

$$\varsigma_p = \frac{N_o \rho(S)}{A(S)} a_p Z^4(S) \tag{16}$$

and

$$\varsigma_c = \frac{N_o \rho(S)}{A(S)} a_c Z(S) \tag{17}$$

where

ς_p: spatial dependency for photoelectric & Rayleigh effects

ς_c: spatial dependency for Compton & Rayleigh effects

We therefore arrive at the abbreviated equations:

$$\mu_p(E,S)=\varsigma_p f_p(E) \tag{18}$$

and

$$\mu_c(E,S)=\varsigma_c f_c(E) \tag{19}$$

The following well known equation describes the x-ray intensity as it is attenuated on passing through a material:

$$I(E)=I_o(E)\cdot e^{-\int \mu(E,S)ds} \tag{20}$$

where

I : final intensity

I_o : initial intensity

From equation 20, the total x-ray beam attenuation can be calculated using the natural log:

$$\int_t \mu(E,S)ds=-\ln\left(\frac{I}{I_o}\right) \tag{21}$$

Remembering that the total attenuation is the sum of two components (equation 3) then:

$$\int_t \mu(E,S)ds=\int_t [\mu_p(E,S)+\mu_c(E,S)]ds \tag{22}$$

For the purpose of simplification let

$$L(E)=\int_t \mu(E,S)ds \tag{23}$$

Equation (22) can then be abbreviated in the following manner using equations 18 and 19:

$$L(E)=f_p(E)\int_t \varsigma_p ds+f_c(E)\int_t \varsigma_c ds$$
$$L(E)=f_p(E)L_p+f_c(E)L_c \tag{24}$$

where

L_p and L_c : line integrals along the same ray path which depend solely on the material properties of the object

It is at this point that dual-energy analysis is introduced. The photoelectric and compton components are not yet known therefore two sets of equations are required in order to solve the problem as a set of linear equations. To obtain the two equations a target is radiated with two energies (E_{lo} and E_{hi}).

$$L(E_{lo})=f_p(E_{lo})L_p+f_c(E_{lo})L_c$$
$$L(E_{hi})=f_p(E_{hi})L_p+f_c(E_{hi})L_c \tag{25}$$

where

$L(E_{lo})$ and $L(E_{hi})$: are collections of ordered points in two separate two images.

Note: *in this situation, the greatest degree of linear independence between the two*

equations must be achieved.

If the set of equations (25) is seen as a matrix, then independency can be achieved between the two equations, by ensuring that the Jacobian is, as follows,

$$J=\det\begin{pmatrix}\frac{\partial L(E_{lo})}{\partial L_p} & \frac{\partial L(E_{lo})}{\partial L_c}\\ \frac{\partial L(E_{hi})}{\partial L_p} & \frac{\partial L(E_{hi})}{\partial L_c}\end{pmatrix} \tag{26}$$

is non-zero.

It must also be well conditioned (stable) so small changes in the input must produce only small changes in the output.

As explained, the high and low energy images $L(E_{hi})$ & $L(E_{lo})$, can be separated by solving the "two equations-two unknowns" shown in equation 25, to produce two more fundamental images, one proportional to the density of the projected material (Compton, equation 15), and one proportional to the product of the density and the cube of the atomic number of the projected material (photoelectric, equation 14).

$$L(E_{lo}),L(E_{hi})\rightarrow L_p,L_c \tag{27}$$

where L_p and L_c are known as the basis images, and can be manipulated linearly to produce cancellation or to determine the average atomic number.

Using Linear Manipulation for Cancellation

$$R=k_1L_p+k_2L_c \tag{28}$$

where

R : a point in residual image

k_1 and k_2 : variables chosen by operator

Consider one overall material, (in this instance aluminum subjected to corrosion) where the x-ray operator is trying to nullify the aluminum in order to increase the contrast:

$$\begin{aligned} R&=k_1[L_p(Al)+L_p(res)]+k_2[L_c(Al)+L_c(res)] \\ R&=[k_1L_p(Al)+k_2L_c(Al)]+[k_1L_p(res)+k_2L_c(res)] \end{aligned} \tag{29}$$

where

res: residual basis image

If an operator selects the variables so that:

$$\frac{k_2}{k_1}=-\frac{L_p(Al)}{L_c(Al)}\propto\frac{\rho Z^3}{\rho} \tag{30}$$

then the aluminum would be cancelled at the point R

Also, by remembering the following relationship:

$$\frac{k_2}{k_1}\propto Z^3 \tag{31}$$

the average atomic number of a substance can be found.

DISTRIBUTION

REPORT NUMBER:	DREP Technical Memorandum 94-05
TITLE:	Dual Energy Radiography: A Potential Corrosion Detection Technique
AUTHOR:	J.D. Leblanc and R.D. Finlayson
DATED:	February 1994
SECURITY GRADING:	UNCLASSIFIED

1 - DSIS Report Collection

1 - CEM
1 - DEMPS
1 - DGRD Ops

1 - DGAEM
1 - DGMEM
1 - DGLEM

1 - AIRCOM
2 - DAS Eng
1 - AMDU
1 - QETE

5 - DREP

SECURITY CLASSIFICATION OF FORM
(highest classification of Title, Abstract, Keywords)

DOCUMENT CONTROL DATA

(Security classification of title, body of abstract and indexing annotation must be entered when the overall document is classified)

1 ORIGINATOR (the name and address of the organization preparing the document. Organizations for whom the document was prepared, e.g. Establishment sponsoring a contractor's report, or tasking agency, are entered in section 8.)

Defence Research Establishment Pacific
FMO Victoria, BC
V0S 1B0

2. SECURITY CLASSIFICATION (overall security classification of the document. including special warning terms if applicable)

UNCLASSIFIED

3 TITLE (the complete document title as indicated on the title page. Its classification should be indicated by the appropriate abbreviation (S,C or U) in parentheses after the title.)

Dual Energy Radiography: A Potential Corrosion Detection Technique

4 AUTHORS (Last name, first name, middle initial)

Leblanc, SLt J.D. and Finlayson, Capt R.D.

5 DATE OF PUBLICATION (month and year of publication of document)	6a. NO. OF PAGES (total containing information. Include Annexes, Appendices, etc.)	6b. NO. OF REFS (total cited in document)
February 1994	40	18

7 DESCRIPTIVE NOTES (the category of the document, e.g. technical report, technical note or memorandum. If appropriate, enter the type of report, e.g. interim, progress, summary, annual or final. Give the inclusive dates when a specific reporting period is covered.)

DREP Technical Memorandum 94-05

8. SPONSORING ACTIVITY (the name of the department project office or laboratory sponsoring the research and development. Include the address.)

DAS Eng 6-2, NDHQ, Ottawa, Ontario, K1A 0K2

9a. PROJECT OR GRANT NO. (if appropriate, the applicable research and development project or grant number under which the document was written. Please specify whether project or grant)	9b. CONTRACT NO. (if appropriate, the applicable number under which the document was written)

10a. ORIGINATOR'S DOCUMENT NUMBER (the official document number by which the document is identified by the originating activity. This number must be unique to this document.)	10b. OTHER DOCUMENT NOS. (Any other numbers which may be assigned this document either by the originator or by the sponsor)
DREP TM 94-05	

11. DOCUMENT AVAILABILITY (any limitations on further dissemination of the document, other than those imposed by security classification)

(X) Unlimited distribution
( ) Distribution limited to defence departments and defence contractors; further distribution only as approved
( ) Distribution limited to defence departments and Canadian defence contractors; further distribution only as approved
( ) Distribution limited to government departments and agencies; further distribution only as approved
( ) Distribution limited to defence departments; further distribution only as approved
( ) Other (please specify):

12. DOCUMENT ANNOUNCEMENT (any limitation to the bibliographic announcement of this document. This will normally correspond to the Document Availability (11). However, where further distribution (beyond the audience specified in 11) is possible, a wider announcement audience may be selected.)

13. ABSTRACT (a brief and factual summary of the document. It may also appear elsewhere in the body of the document itself. It is highly desirable that the abstract of classified documents be unclassified. Each paragraph of the abstract shall begin with an indication of the security classification of the information in the paragraph (unless the document itself is unclassified) represented as (S), (C), or (U). It is not necessary to include here abstracts in both offical languages unless the text is bilingual).

The recent demand for extending the service life of aircraft fleets well beyond the original design life has made the early detection of corrosion in aircraft a major concern. Consequently, many nondestructive techniques to improve corrosion detection are being investigated. One potential method is known as "Dual-Energy" (DE) radiography and is based on the collection of two different radiation energy spectra. This is achieved by producing two distinct radiation energies, either by changing the radiation source energy, or by filtering and collecting the radiation from one source via filtered detectors. The information collected from the different spectra can then be combined to form a digital image that can be used to determine an unknown substance or to remove the effect of a particular substance to improve contrast.

In this report the theory and concepts of DE are examined and a number of existing systems are discussed. Finally, the possibility of implementing a DE system at the Defence Research Establishment Pacific is investigated.

14. KEYWORDS, DESCRIPTORS or IDENTIFIERS (technically meaningful terms or short phrases that characterize a document and could be helpful in cataloguing the document. They should be selected so that no security classification is required. Identifiers, such as equipment model designation, trade name, military project code name, geographic location may also be included. If possible keywords should be selected from a published thesaurus. e.g. Thesaurus of Engineering and Scientific Terms (TEST) and that thesaurus-identified. If it is not possible to select indexing terms which are Unclassified, the classification of each should be indicated as with the title.)

aerospace
Compton
corrosion
dual energy
non-destructive
photoelectric
physics
radiography
X-rays

4/18

#146068

NO. OF COPIES NOMBRE DE COPIES	COPY NO. COPIE N°	INFORMATION SCIENTIST'S INITIALS INITIALES DE L'AGENT D'INFORMATION SCIENTIFIQUE
1	1	JB

AQUISITION ROUTE / FOURNI PAR ▶ DREP

DATE ▶ 04 Oct 94

DSIS ACCESSION NO. / NUMÉRO DSIS ▶ 95-00097

National Defence / Défense nationale

DND 1158 (6-87)

PLEASE RETURN THIS DOCUMENT TO THE FOLLOWING ADDRESS:

DIRECTOR
SCIENTIFIC INFORMATION SERVICES
NATIONAL DEFENCE
HEADQUARTERS
OTTAWA, ONT. - CANADA K1A 0K2

PRIÈRE DE RETOURNER CE DOCUMENT À L'ADRESSE SUIVANTE:

DIRECTEUR
SERVICES D'INFORMATION SCIENTIFIQUES
QUARTIER GÉNÉRAL
DE LA DÉFENSE NATIONALE
OTTAWA, ONT. - CANADA K1A 0K2